J Nanostruct 16(3): 3635-3649, Summer 2026

RESEARCH PAPER

Integrated Characterization of Deposited Dust and Atmospheric Particulate as a Micro/Nano Matter Across Urban, Rural, and Industrial Environments in Hillah City, Iraq

*Najla Alaa Jabbar *, Hussein Aliwy Hassan AL-Keriawy*

Environmental Pollution Department, Collage of Environmental Sciences, Al-Qasim Green University, Babylon, 51013, Iraq

ARTICLE INFO

Article History:
Received 17 March 2026
Accepted 18 June 2026
Published 01 July 2026

Keywords:
Atmospheric Pollution
Dust and Suspended Particles
Micro/nano matter

ABSTRACT

This study provides an integrated assessment of the spatial distribution, physical and chemical characteristics and potential sources of deposited and suspended particulate matter in Hillah City, Babylon Governorate, Iraq. Dust samples were collected from urban, rural, and industrial sites between October 2024 to June 2025. The study measurement of dust deposition rate, concentration of particulate matter ($PM_{2.5}$ and PM_{10}), size distribution, and meteorological conditions. extensive morphological, mineralogical, and geochemical evaluations were performed using (SEM), (XRD), and (XRF) to determine particle morphology, mineral phases, and element composition. Dust and airborne particulate matter deposited onto surfaces have large seasonal and spatial variability. The higher average dust deposition value (g/m^2) at the industrial site (86.7–3.68), following the rural sites (46.24–8.50). Also, the urban sites recorded values ranging from (37.40–4.40). In contrast, the highest PM concentrations ($\mu g/m^3$) were found in the urban environment, where $PM_{2.5}$ was (98.22– 11.41) and PM_{10} was (158.21–17.69). Slightly lower concentrations were present in the rural site (83.31– 27.48 for $PM_{2.5}$ and 125.24–41.86 for PM_{10}) while the lowest levels were at the industrial site (74.13– 14.97 for PM2.5 and 94.21– 22.80 for PM_{10}). Statistical analyses found a strong positive correlation between $PM_{2.5}$ and PM_{10} concentrations; however, both PM concentrations had negative correlations with temperature and wind speed, thus illustrating how meteorological variables influence the dispersing of particulate matter. Mineralogical results from SEM-EDS suggest quartz and calcite as predominant mineral types, confirming that there are considerable amounts of crustal contributors to the measurements.

How to cite this article
Alaa Jabbar N., Aliwy Hassan AL-Keriawy H. PIntegrated Characterization of Deposited Dust and Atmospheric Particulate as a Micro/Nano Matter Across Urban, Rural, and Industrial Environments in Hillah City, Iraq. J Nanostruct, 2026; 16(3):3635-3649. DOI: 10.22052/JNS.2026.03.054

INTRODUCTION

Air pollution represents one of the most critical environmental challenges of the twenty-first century, causing approximately seven million premature deaths annually worldwide [1]. Dust is a natural phenomenon significantly affecting climate systems, air quality, and public health [2,3]. In Iraq, prevailing climatic conditions

* *Corresponding Author Email: najlaa@environ.uoqasim.edu.iq*

high temperatures, low precipitation, and increased evaporation have made dust a major environmental concern, with drought and soil erosion serving as primary natural sources [4]. Particulate matter (PM), particularly PM_{10} and $PM_{2.5}$, represents one of the most hazardous air pollutants due to its direct association with respiratory and cardiovascular diseases [5]. Particle size distribution (PSD) determines particle behavior regarding suspension, deposition, and respiratory penetration [6]. Beyond physical characteristics, dust contains heavy metals resistant to biodegradation and bio accessible in the human body, potentially causing neurological disorders, kidney and liver diseases, and cancer [7,8]. These metals originate from both natural sources (dust resuspension) and anthropogenic activities (vehicle emissions, industrial processes) [9,10]. Due to limited studies in Hillah city integrating multiple analytical techniques, this comprehensive investigation aims to: (1) measure PM_{10} and $PM_{2.5}$ concentrations and dust deposition rates; (2) examine particle morphology using SEM; (3) identify mineral phases using XRD; (4) determine heavy metal concentrations using XRF; and (5) correlate findings with meteorological factors and anthropogenic activities.

MATERIALS AND METHODS

Study Area and Sampling Sites

Hillah City, the administrative center of Babylon Governorate, is located approximately 100 km south of Baghdad in central Iraq. The city has experienced rapid urban expansion, population growth, and increasing industrial activities. The climate is hot desert, characterized by extremely

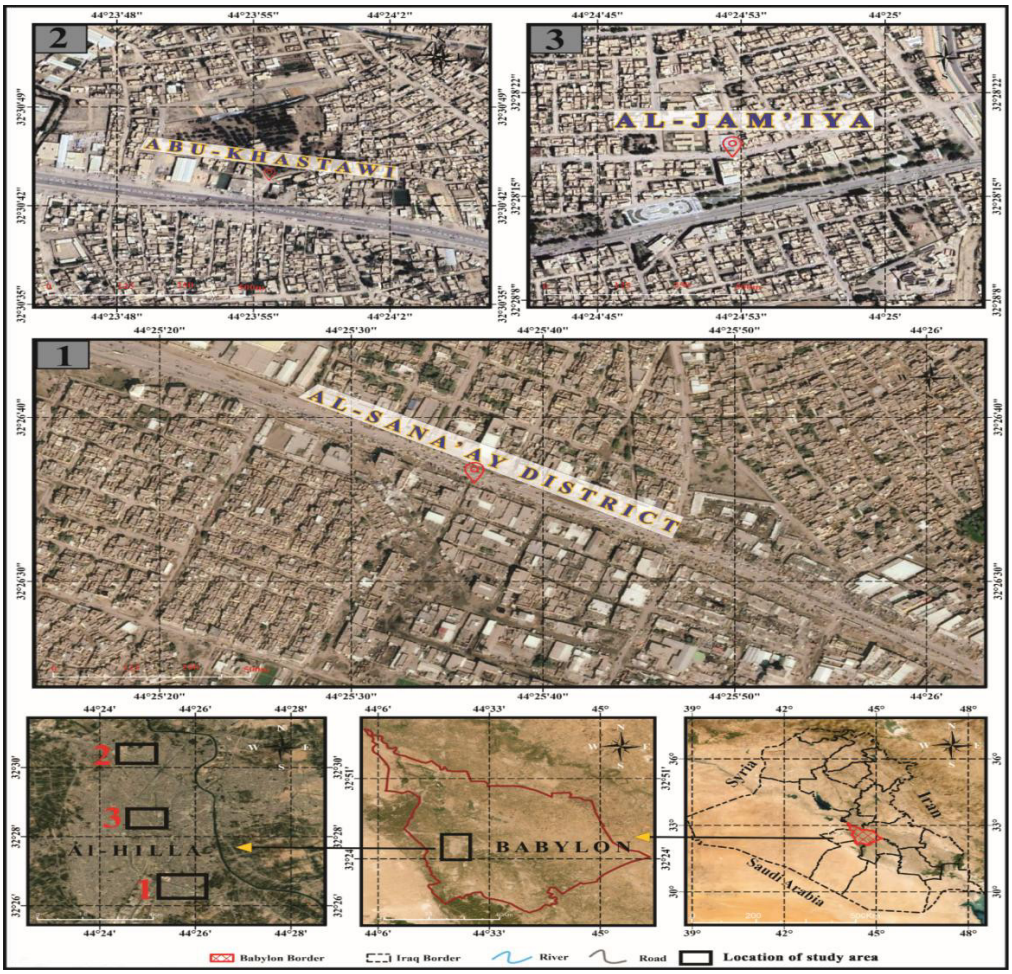

Fig. 1. Location Map of the study area and sampling sites.

high summer temperatures, mild winters, and low annual precipitation [11].

Description of Sampling Sites

An Urban Area (AL-Jam'iya District): This is a specific archetype of an urban dense residential and commercial area having high traffic flow, commercial centers, and daily anthropogenic activities. Coordinates: 32.470653 N, 44.414645 E.

Site 2 — Rural Area (Abu–Khastawi): This site provided a rural and agricultural environment with vegetation cover, farming activities, and very few industries. It's located away from center. Coordinates: 32.512578 N, 44.398056 E.

Industrial Areas (Industrial zone): This place shows a typical industrial environment with vehicle engine maintenance workshops and other minor industrial activity, which forms a significant source of pollutants emission. Coordinates: 32.470653 N, 44.427247 E (Fig. 1).

Dust Sampling and Deposition Rate

Monthly samples of deposited dust were collected from October 2024 to June 2025 by means of pipe-less cylinders deposited at heights to minimize their direct contamination. The samples were weighed in the laboratory on a digital scale sensitive to micrograms after having

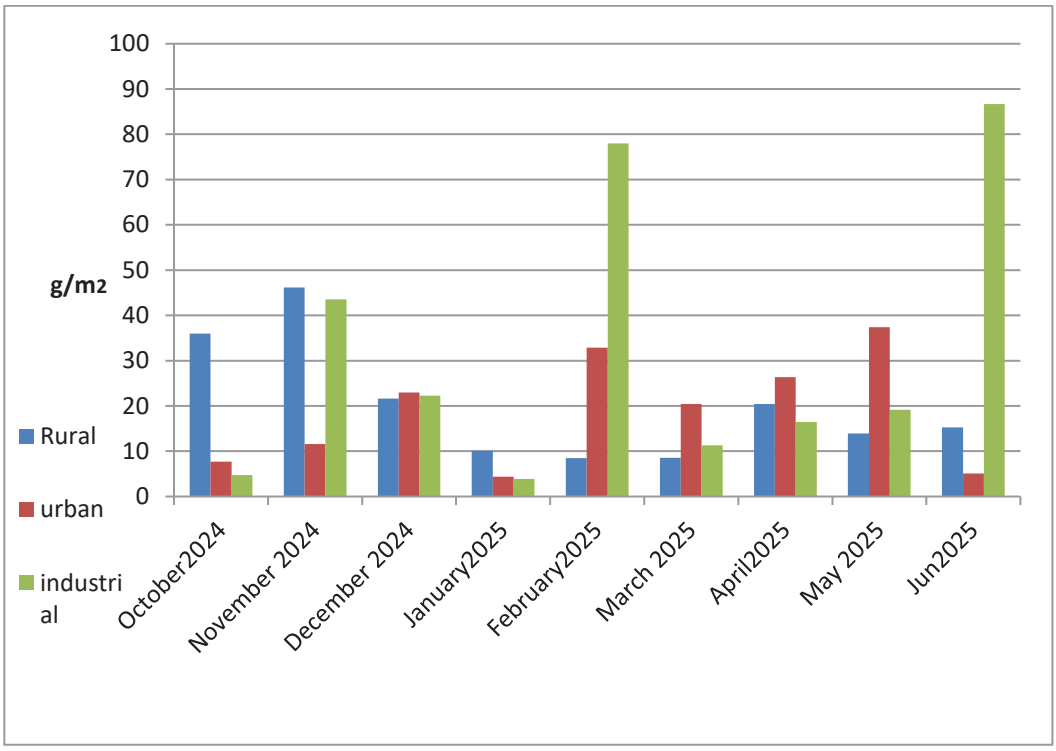

Fig. 2. Monthly values of deposited dust (g/m²).

Table 1. Descriptive statistics of dust deposition rates (g/m²) in the study area.

Area	Min g/m²	Max g/m²	Mean ± SD g/m²	Correlation with temperature	Correlation with wind speed	Correlation with Humidity
Industrial	3.68	86.70	31.77 ± 31.03	0.058	0.088	-0.120
Rural	8.50	46.24	20.06 ± 13.07			
Urban	4.40	37.40	18.75 ± 12.21			

also been air-dried. DDR (g m^{-2} d^{-1}) is a dust deposition rate calculated by equation.

$$DDR = \frac{W_2 - W_1}{A} \quad (1)$$

Where, W_1 = Weight of the cylinder before collection. W_2 = Weight of the cylinder after collection. A = area of the cylinder base (m^{-2}).

Measurement of Particulate Matter (PM_{10} and $PM_{2.5}$)

Concentrations of PM_{10} and $PM_{2.5}$ were measured at the selected sites using a portable air quality monitoring device (Tem Top). Measurements were conducted at fixed time intervals during the study (from October 2024 to June 2025) to ensure consistency and comparability among the studied areas.

Particle Size Distribution (PSD)

Particle size distribution of the deposited dust samples was analyzed to determine the relative contribution of fine and coarse particles and to evaluate the dominant particle size fractions.

Scanning Electron Microscopy (SEM)

The morphological characteristics of the dust particles, including shape and surface texture, were examined using a scanning electron microscope (SEM) at the laboratories of the University of Babylon. (Device model: ESCAN VEGA 3, Czech Republic).

X-ray Diffraction (XRD)

The mineralogical composition of the deposited dust samples was identified using X-ray diffraction (XRD) analysis to determine the crystalline phases present. (Device model: XRD-6000, Shimadzu, Japan).

X-ray fluorescence

The X-ray fluorescence (XRF) technique was used to determine the concentrations of heavy metals in the deposited dust samples. After drying and grinding, the samples were placed on

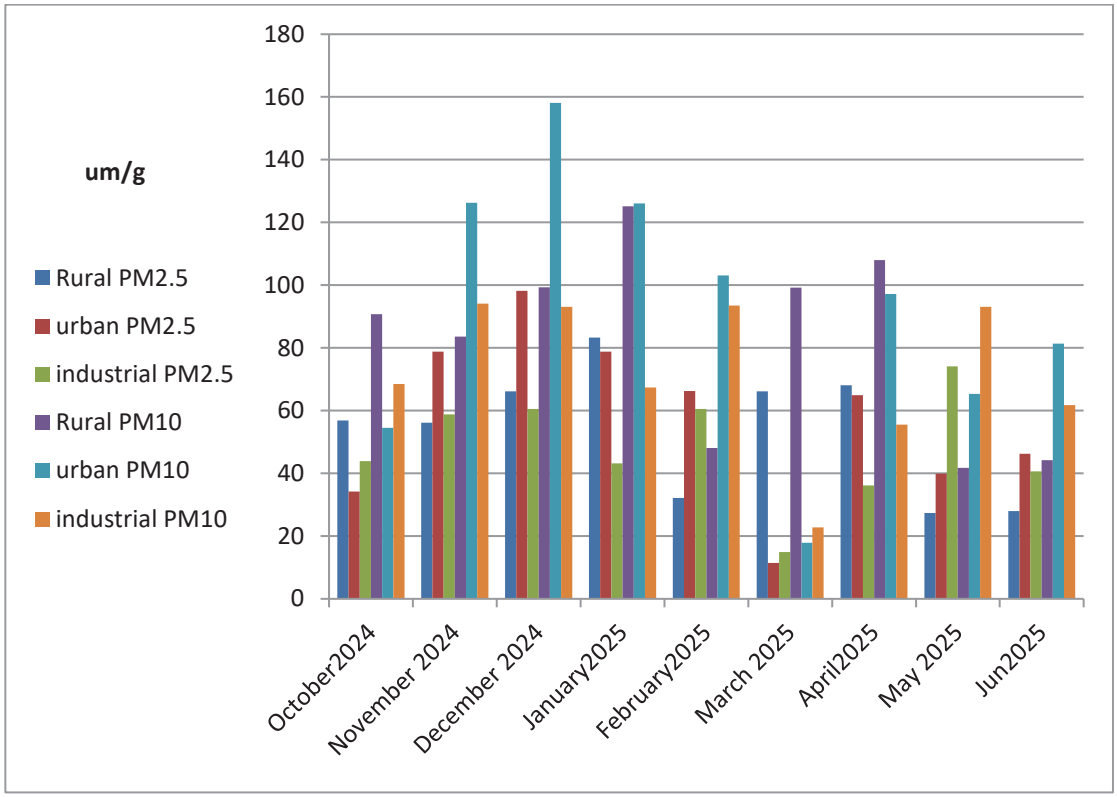

Fig. 3. Monthly Concentration Values of (PM_{10}, $PM_{2.5}$).

a disc-shaped holder with a diameter of about (3 cm). The weight of the analyzed samples ranged from 3 to 5 g. The analysis was carried out at the laboratories of the Scientific Research Authority, Ministry of Higher Education and Scientific Research, Baghdad. (Device model: XEPOS, SPECTRO Analytical Instruments, Germany).

RESULTS AND DISCUSSION

Dust deposition

The result of dust deposition showed noticeable spatial variation in all sites. Especially in monthly value, since the industrial site recorded the highest dust deposition rate in June (86.70 g/m^2) and the lowest value (3.86 g/m^2) in January in the same area. (Fig. 2)

Descriptive statistics indicated that the industrial site exhibited the highest average dust deposition rate (31.77 ± 31.03 g/m^2), followed by the rural site (20.06 ± 13.07 g/m^2), whereas the urban area recorded the lowest value (18.75 ± 12.21 g/m^2). The descriptive statistics of the deposition rates for the studied areas are summarized in Table 1.

Statistical analysis revealed high variability in dust deposition within the industrial area, while relatively stable values were observed in the

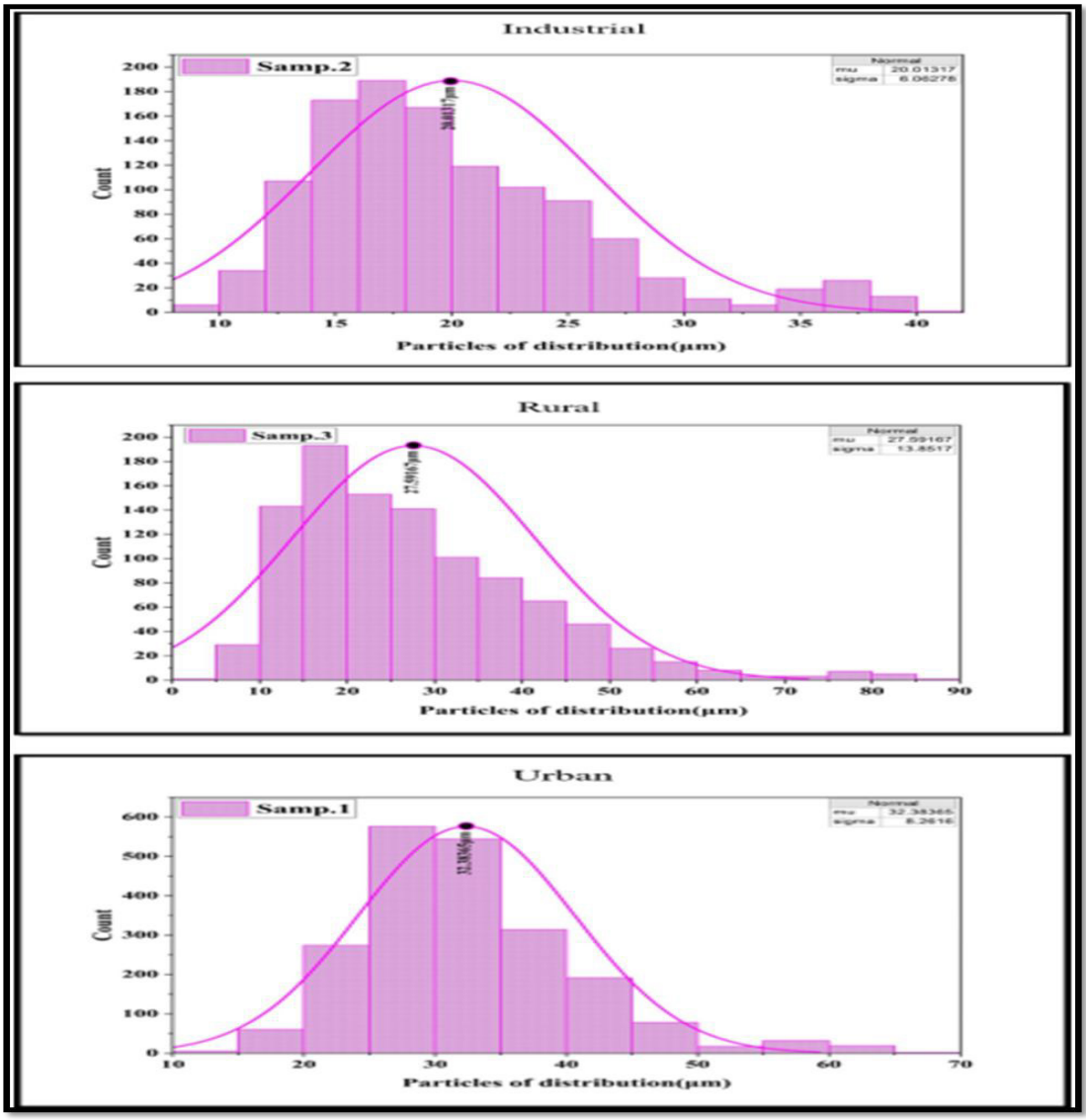

Fig. 4. Particle size distribution of deposited particles in the studied areas.

rural and urban areas. Weak negative correlation was found between dust deposition and relative humidity, whereas weak positive correlation was observed with air temperature and wind speed, with no statistically significant differences. This indicated that meteorological factors played a secondary role in controlling dust deposition during the study period. The elevated dust deposition in the industrial area can be attributed to local anthropogenic activities, such as vehicle movement on unpaved roads and emissions from nearby workshops, which are considered major sources of dust in industrial environments [12]. In contrast. The lower dust levels in the rural area may be associated with vegetation cover and soil moisture, which reduce dust emissions [13]. The urban area recorded the lowest dust deposition rate, likely due to paved roads, urban planning,

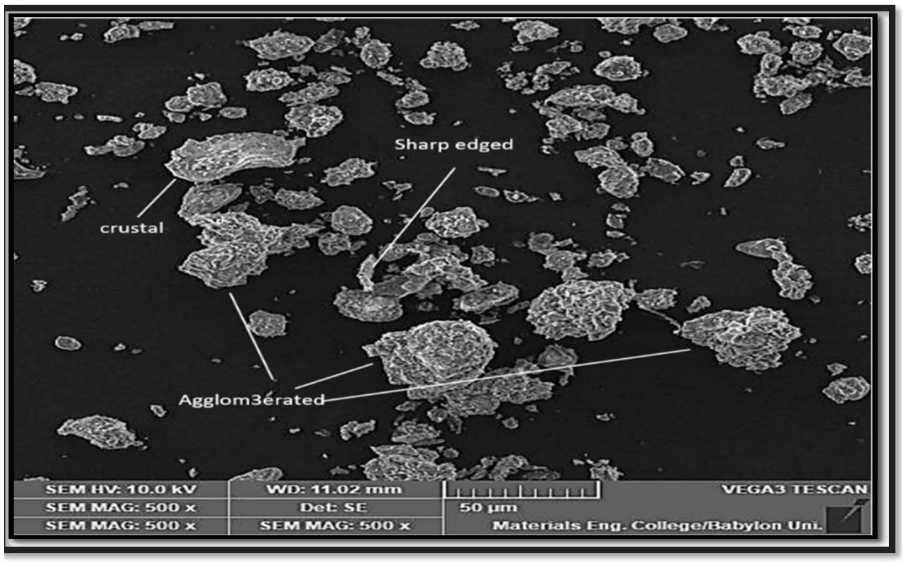

Fig. 5. SEM images of the agricultural area.

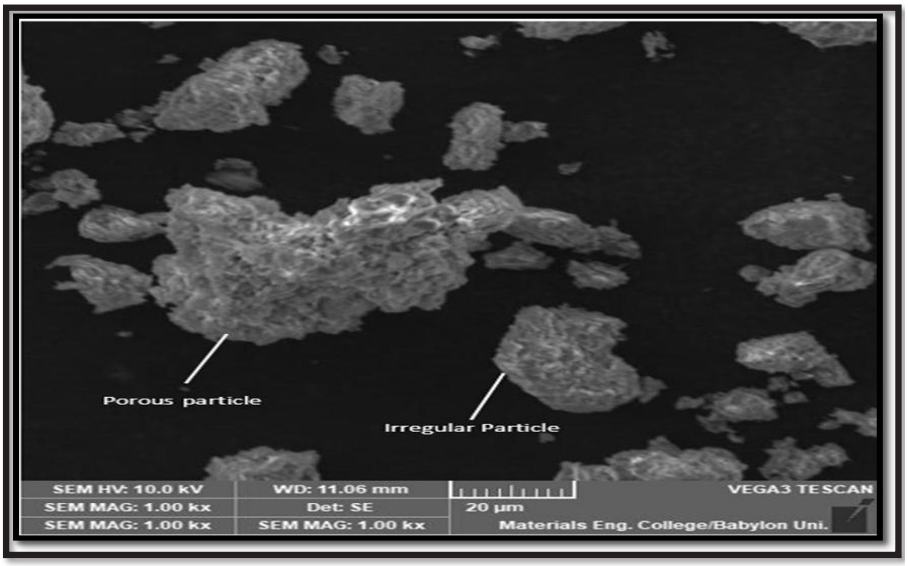

Fig. 6. SEM images of the urban area.

and limited industrial activities, as well as the presence of green spaces, which contributed to reducing dust emissions [14]. Overall, the results suggest that local anthropogenic sources play a more dominant role in dust accumulation than climatic factors, particularly in the industrial area, consistent with previous studies [12,15].

Particulate matter (PM_{10} and $PM_{2.5}$)

The descriptive statistics of PM_{10} and $PM_{2.5}$ revealed clear spatial and seasonal variability across the study sites. Higher concentrations were generally recorded during the winter months, while lower values predominated in summer. For $PM_{2.5}$, the urban area recorded the highest mean concentration. And the recorded concentration ranged from (98.20 to 11.040 µg/m^3) in the urban area, at December 2024 and march 2025 respectively, and (83.30 to 27.40 µg/m^3) at January 2025 and May 2025 in the rural area, respectively, while (74.10 to14.90 µg/m^3) at May 2025 and march 2025 in the industrial area. Respectively, with means (57.64 ±26.92 µg/m^3), in urban area, followed by the rural area (53.82 ±20.08 µg/m^3), whereas the industrial site showed the lowest mean value (48.06 ±17.47 µg/m^3).

The PM_{10} recorded monthly value ranges were (158.10 to 17.90 µg/m^3). for the urban area at December 2025 and March 2025, respectively, and (125.10 to 41.80 µg/m^3) at January 2025 and May 2025, respectively, in the rural area, while in industrial areas (94.10 to 22.80 µg/m$^{3)}$ at November2024 and March 2025, respectively, Similarly, PM_{10} showed the highest mean concentration in the urban area (92.21 ±42.69 µg/m^3), followed by the rural site (82.24 ±30.36 µg/m^3). While the industrial area recorded the lowest mean value (72.24 ±24.20 µg/m^3). (See Fig. 3).

The result of the particle size distribution of dust particles showed clear differences among the urban agricultural, and industrial areas. The urban area recorded the highest mean particle size, reaching (32.38 ±8.26µm), whereas the industrial area exhibited the lowest mean particle size of

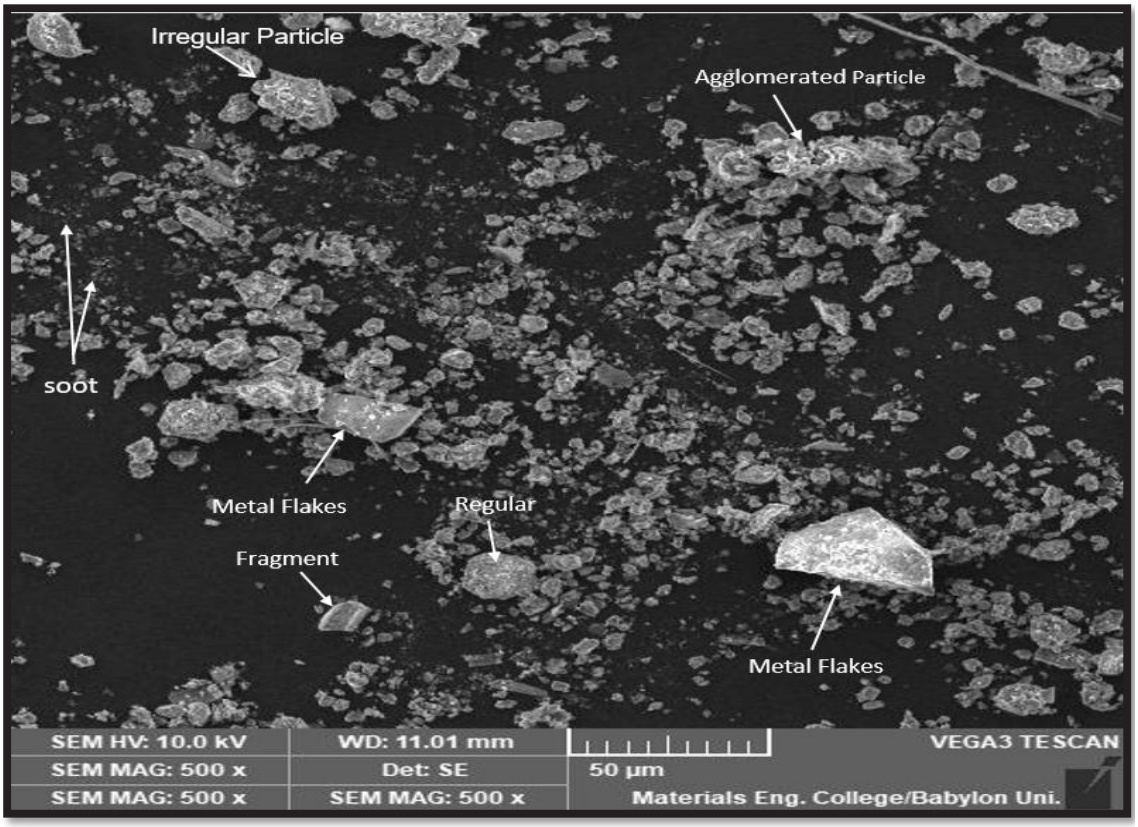

Fig. 7. SEM images of the industrial area.

(20.01 ±6.06 µm), The agricultural area showed an intermediate value between the two areas with a mean particle size of (27.59 ±13.85 µm). The dominant particle size of deposition dust ranged from 10 µm to 70 µm across the three sites. The objective of analyzing the particle size distribution of dust particles is to clarify the spatial differences in particle sizes among urban, agricultural, and industrial sites and to relate them to the nature of the sources and dominant activities at each site. The particle size distribution in the urban area indicates the dominance of relatively large particles as the distribution curve extends toward higher values, reaching up to 70 µm this reflects the prevalence of coarse particles. This suggests soil particles resulting from dust suspension and daily human activities with traffic movement being the primary source in most cases [16]. In contrast, the industrial area was characterized by the presence of smaller-sized particles compared to the urban and agricultural areas. This can be attributed to the influence of industrial activities, which generated finer and relatively homogeneous particles as a result of combustion processes and mechanical abrasion enabling these particles to remain suspended in the air for longer periods. Meanwhile, the particle size distribution in the agriculture area showed intermediate values between the two areas. This pattern is attributed to soil fragmentation, wind erosion, and agricultural activities, which generated particles of natural origin. The study of Huang illustrate that the wind contributes to an increase in dust particulate size by enhancing emission rates and reducing dust deposition [17]. The analysis of variance concerning standard deviation values confirmed that there were multiple sources of particles at all three sites. The rural area possessed the highest standard deviation, indicating that there were a variety of sources and that there was heterogeneity in soils [18], whereas the industrial site had the lowest standard deviation, indicating that there was homogeneity among the sources due to the industrial process. A characterization of particle sizes revealed that there was a distinct spatial gradient regarding size of particles: the largest sizes were found in the urban area, somewhat smaller in the agricultural area, and then the smallest sizes in the industrial area. These results are consistent with the findings of [15], who found that most of the particles at urban and agricultural locations comprised mostly large particles, whereas the majority of particles found at industrial sites consisted of smaller particles (Fig. 4).

Scanning Electron Microscope (SEM)

The result of the (SEM) showed the presence of various shapes of deposited dust particulate, including spherical (rounded), flat, elongated, and irregular particles with sharp edges and metallic flakes. This indicates that the deposition dust particles consist of a heterogeneous mixture of different morphologies as shown in Figs. 5-7.

Dust particle morphology analysis using SEM by site has shown different morphological characteristics. The morphology of dust particles was irregular and heterogeneous due to different sources, meteorological conditions, the length of time the particles spent in the atmosphere, and the elemental make-up of the particles [18,19]. The irregular platy-shaped particles that had sharp edges and rough surfaces were primarily attributed to weathering of the primary crust and the effects of weathering from wind erosion [20] and the effects of human activities, including construction sites and road dust from vehicles [21]. Very small round, smooth spherical-shaped particulate matter was found to be representative of soot from the emission of vehicles and combustion [22,23]. Highly porous particles containing carbon from agricultural or waste burning have high adsorption capacity and ability to aggregate over large areas [24,25] were also seen SEM analysis from the industrial sites identified metal particles and broken particles produced from mechanical processes that are produced through diligence in the Workshop. The results of this research identified two major categories of particles, anthropogenic round shiny particles created from combustion and natural irregular rough surface particles that have been formed from geological and biological sources [26] and corroborates with the findings of [20], that particle morphology represents the characteristics and origin of the source of the particle.

Mineralogical identification of deposited dust particles

X-ray diffraction (XRD) analysis was conducted on the total deposited dust samples from the three study sites to identify the mineralogical composition. Calcite ($CaCO_3$) and Quartz (SiO_2) were identified in all sites. In contrast, less

common phases in the atmospheric dust were preliminarily identified based on peak matching according to standard reference, (ICDD reference patterns) (Table 2).

X-ray diffraction (XRD) tests indicated all locations had calcite and quartz indicating that there are natural crustal components present in the atmospheric dust as shown in Fig. 8.

Calcite is the major mineral within carbonate-rich soils, so the presence of this mineral in atmospheric dust is not abnormal; however, its presence may also be attributed to cement-related pollution since it is widely used in many industries, and its environmental effects through chemical weathering [27,28]. Quartz is resistant to physical and chemical weathering and is therefore used as a reliable index to identify crustal dust from natural sources including soil re-suspension, dust storms, and vehicular activity, but peak intensity can vary by site [29]. The feldspar phase, Albite Calcine Low ($Al_{1.16}Ca_{0.16}Na_{0.84}O_8Si_{2.84}$), was discovered as a result of soil re-suspension and rock fragmentation. Lead Calcium Zirconium Oxide ($Ca_{0.3}O_3Pb_{0.6}5Zr$), which served as an indicator of anthropogenic pollution caused by vehicle emissions and brake operations [30,31], was detected in urban samples Molybdenum nitride (Mo_2N) was present in industrial dust samples, indicating a chemical or thermal interaction resulted from molybdenum sources with nitrogen-containing gases from industrial workshop processes such as welding, polishing, or thermal spraying [32]. An intermetallic alloy phase ($GaMnNi_2$), which was formed under high vacuum at elevated temperatures, also appeared in industrial samples, confirming that anthropogenic industrial emissions are likely causing the presence of this alloy or suspending metallic particles. In rural areas, rubidium iodate ($RbIO_3$) was found which is uncommon and forms through the adsorption of rubidium that occurs naturally in clay-rich soils and of mobile iodate anions by wind re-suspension of soil particles into the atmosphere [33-35]. In addition to rubidium iodate, strontium chromate (Sr_2CrO_4), which is known to be a carcinogen, was identified as a result of aerosolized dispersal of paint particles through the air during the process of painting as a means of providing protection from corrosion by using corrosion resistant paint [36,37]. The results of this study are consistent with the work of [38], who reported that calcite, quartz, albite, and dolomite were sourced from natural geological

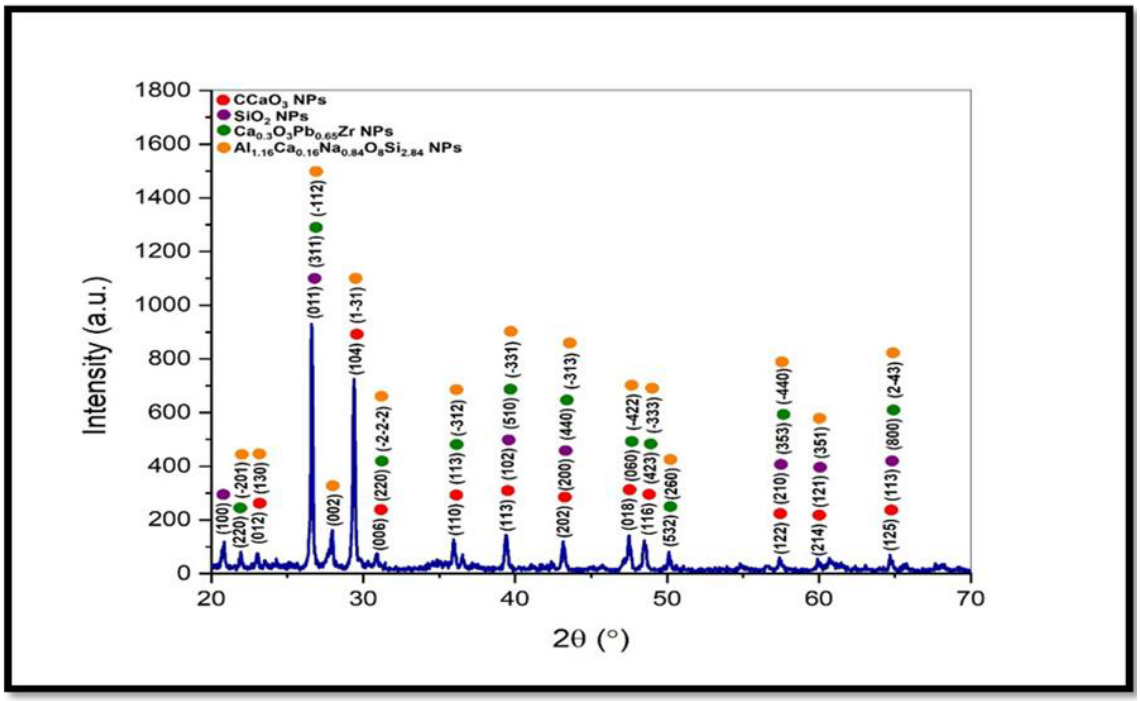

Fig. 8. X-ray diffraction patterns of deposited dust particles in urban areas.

processes associated with rock weathering and that illite, hematite, and montmorillonite were sourced from anthropogenic activities such as construction and industrial emissions.

Heavy Metal Interpretation (XRF Analysis)
Spatial Variation

Results of the analysis of spatial statistics showed a clearly defined variation in concentrations of heavy metals amongst the various measurement sites included in this study. The urban area had the greatest mean concentration at 110.91 + 195.33 with the industrial area second at 93.28 + 150.10. In contrast, the rural location had the lowest average concentration at 88.43 + 176.98. The high standard deviation values indicate significant heterogeneity of heavy metal concentration across each site, most likely due to the non-uniform distributions of heavy metals and differing emission sources from anthropogenic activities rather than consistent

Table 2. Phase identification based on qualitative peak matching using X'Pert High Score software.

Area	Phase name	Chemical formula	Main peaks (2θ)	ICCDD PDF NO.
Industrial	Calcite	$CaCO_3$	29.3, 39.3, 35.9	01-072-1937
	Quartz	SiO_2	26.6, 50.1, 20.8	01-085-0798
	Molybdenum Nitride	Mo_2N	37.6, 43.0, 45.3	01-075-1150
	Gallium Manganese Nickel	$GaMnNi_2$	43.9, 80.8, 63.9	00-050-1518
Urban	Quartz alpha, syn	SiO_2	26.6, 20.8, 50.1	01-078-1252
	Calcite, syn	$CaCO_3$	29.3, 47.5, 39.3	01-081-2027
	Albite calcian low	$(Na_{0.84}Ca_{0.16})Al_{1.16}Si_{2.84}O_8$	27.9, 27.8, 23.9	01-076-0927
	Lead Calcium Zirconium Oxide	$(Pb_{0.65}Ca_{0.3})ZrO_3$	30.8, 44.1, 54.9	01-086-1116
Agriculture	Calcite	$CaCO_3$	29.4, 48.5, 39.4	01-086-2334
	Quartz	SiO_2	26.6, 20.8, 50.1	01-085-0797
	Rubidium Iodate	$RbIO_3$	27.7, 39.6, 49.1	00-030-1068
	Strontium Chromium Oxide	Sr_2CrO_4	30.8, 44.1, 36.9	00-033-1324

and continuous background sources.

The results depicted in Fig. 9 show significant differences in heavy metal concentrations between study locations and are consistent with descriptive statistics. This demonstrates non-uniform (anisotropic) heavy metal concentration distribution in deposited dust, especially in urban settings, where there's considerable variability of heavy metal concentrations spatially.

The boxplot demonstrates how there is a lot of variability amongst samples due to the wide range of concentrations in each region, as well as due to outlying data points. The boxplot indicates that the boxplot shows some level of uniformity across the sample regions while also exemplifying variabilities through the heavy metal distributions which are indicative of anthropogenic sources, as they originate from a large number of direct and highly varied location sources. Examples of differences that occur between sample locations are also visible on the boxplot through the differences in sample population variability.

Seasonal Variations

Lastly, with respect to seasonal variation in heavy metal concentrations found in deposited dust samples collected during the summer (96.83 ± 180.11) and winter (98.25 ± 169.57) seasons, only minor differences have been observed. In general, the mean concentrations between seasons were relatively equal, however, there is a large amount of variability as indicated by the high standard deviation values. Given that there is so much variability in the heavy metal concentration samples collected between seasons, the probability of significant seasonal variations resulting is very low, as is demonstrated by the data presented in Fig. 10.

Statistical analysis showed differential seasonal behavior of heavy metals in each of the study areas. Higher mean concentrations were recorded for winter (101.16) than for summer (85.40) in the case of industrial areas, which possibly reflects higher industrial activity or less atmospheric dispersion in winter. In urban regions, mean concentrations showed comparatively little difference between summer (113.01) and winter (108.82), indicating stability of the source of emission. On the other hand, the rural region found that summer concentrations were slightly increased (92.09) compared to winter (84.77), which may be related to agricultural activities. This suggests that season effects differ across regions but are minor in comparison to the combined variation in a single season, thus confirming the idea that direct local sources control heavy metal concentration in deposited dust.

There was also no statistically significant difference in mean heavy metal concentration between the three regions according to the Two-

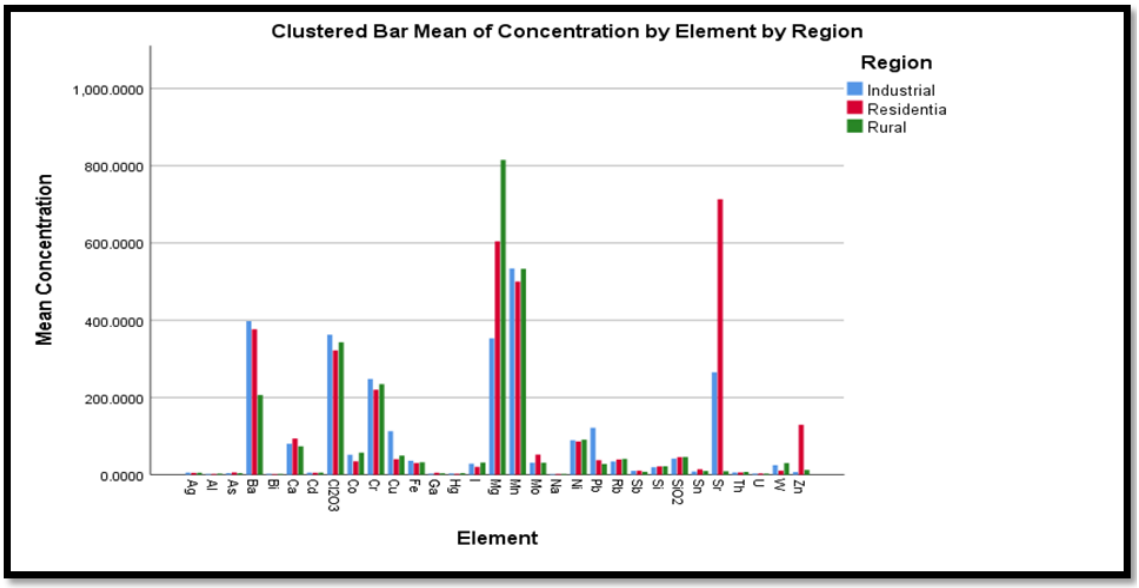

Fig. 9. Spatial variation of heavy metal concentration in the study areas.

Way ANOVA (Region x Season) (Sig =0.757, F=0.279) No significant differences were also seen between summer and winter (Sig = 0.956, F = 0.003). There was also no significant interaction between region × season (Sig = 0.925, F = 0.078). Region, season, and the interaction of region and season had no statistically significant effect of heavy metal concentrations (Sig = 0.982) in the corrected model. The R^2 (coefficient of determinant) was limited (0.004). These results suggest that spatial and seasonal characteristics account for only a quite minimal part of the variation in heavy metal concentrations, suggesting that the levels of heavy metals in deposited dust are more likely driven by nearby local sources or other unexplored variables than by location and season.

The heavy metals concentrated and subjected to mean concentrations show variation in deposited dust samples. The mean concentrations of the elements Mg, Mn, Sr, Ba, and Cr were relatively high, while the mean concentrations of Na, Hg, Cd, Sb, and Sn were extremely low.

The heavy metals distribution in reveals high and low mean concentrations of elements, which confirm the differences in the abundance of the elements. And as further evidence of the statistical analysis results, within dust samples. Certain heavy metals had high standard deviation values (indicating large variation in concentration) and others demonstrated low standard deviation values (indicating relatively stable concentrations) within the time interval between measurements.

As shown in the box plot, heavy metals are exhibited to high dispersion, where most with wide range and some with outliers, confirming high dispersion. Variability with dust samples. Standard error analysis was conducted as a follow-up to assess the accuracy of mean concentrations. Centering and spread are described with mean, and error bars represent standard deviation, respectively (Fig. 11) this file is in the first Proceedings Data.

Source Classification of Heavy Metals

Lithogenic (Natural) Elements

The high concentrations of some elements deposited dust include: Mg, Mn, Sr, Ba, Fe, Ca and Si and SiO_2. This elevation should be normal based on the crustal origin of these elements and their abundance in adsorption-based raser within prophylytic surface soils that were enriched through weathering and erosion of rocks and soils

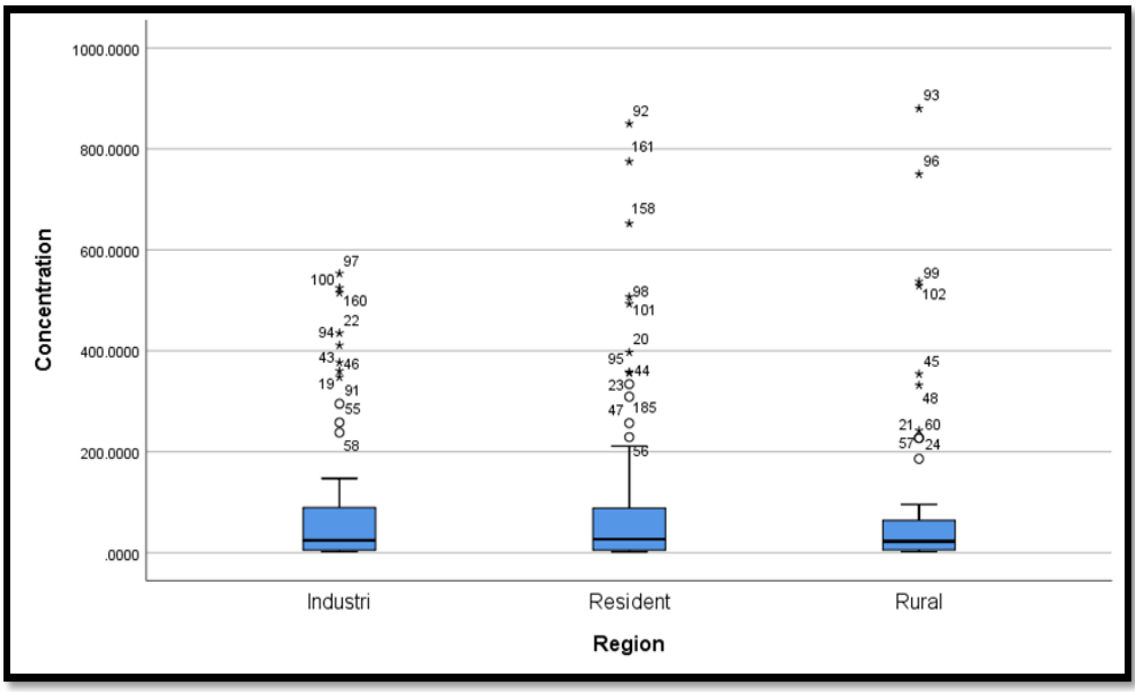

Fig. 10. Box plot of heavy metals in the study areas.

rather than being industrial or anthropogenic polluted [39] [40]. Low average concentrations were recorded for Mn with the exception of the mining regions, and also for two elements, Cu and Ca, which were expected to show a relatively higher mean concentration, which is due to their general abundance in the study areas, except for the mining regions. High standard deviation values relative to each other indicate variation in concentrations, potentially due to climatic factors like wind and dust resuspension. As long as they do not exceed the environmental safety limits, the crustal heavy metals that originate from dust are treated as natural background instead of environmental pollution.

Anthropogenic Elements

Contrarily, anthropogenic variables, exhibiting different concentrations include Pb, Zn, Cu, Ni, Mo, Cd, Sb, Hg, As, Sn, and Co, and their concentrations are significantly controlled by human activities (industrial, traffic, combustion, and construction)· The mean concentrations of many elements recorded relatively high variability revealed in the high standard deviation (a huge fluctuations of samples). Such irregularity is associated with temporally and spatially variable emissions from human activities and is reflected as variability in total columns of Co [41]. Box plot depicted wide ranges and outliers present, which is a hallmark of anthropogenic nature, where emissions tend to be local and sporadic rather than uniform sources [42]. These factors have no national or seasonal pattern and instead rely on local customs. The increased concentrations of these species in settled dust signifies a direct effect of human activities on air quality and the regional environment, which may be of anthropogenic and not geological origin and could contribute to the environmental burden by continued deposition if they are not addressed.

These results are in agreement with [43] who established that Fe, Mn, Co, and Ni in deposited dust are mainly of natural origin, while Pb, Zn, Cd and Cu are closely related to anthropogenic input. Likewise, [44] stated that changes in heavy metal concentrations in Baghdad could be due to environmental fluctuations and several origins

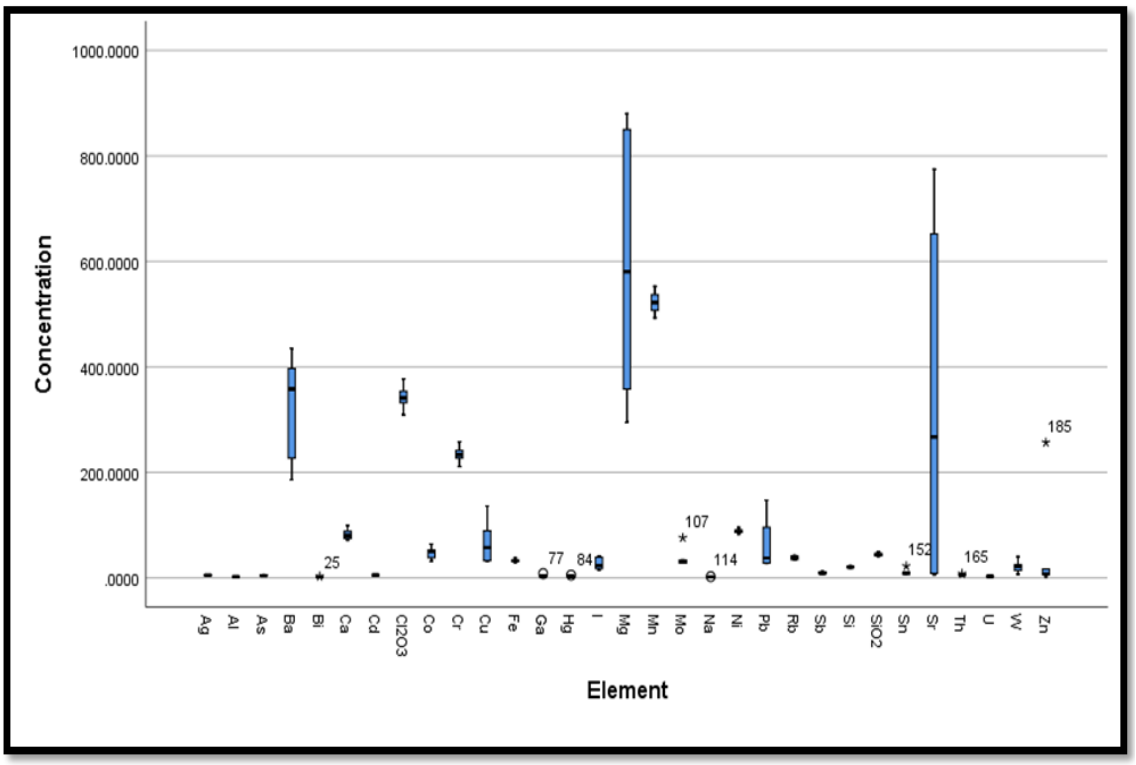

Fig. 11. Box plot of heavy metals.

such as dust storms and patchy plant distribution.

CONCLUSION

This research shows the primary cause of particulate pollution in Hillah City is local source emissions while there is greater spatial than seasonal or meteorological variability. The principal means of depositing these particles are industrial areas due to mechanical processes, unpaved surfaces, and localized emissions. The majority of particulate matter (PM) concentration is found in urban areas with $PM_{2.5}$ and PM_{10} being primarily caused by vehicle emissions/transportation and urban activity. The close relationship between $PM_{2.5}$ and PM_{10} indicates that the two particle sizes come from similar areas and both types have a common atmospheric mechanism for distribution. The particle size distribution has clear environmental separation where the larger particles are derived from resuspension of dust within the urban areas and the smaller ones are from industrial processes. While there are some elemental or chemical composition similarities in the aggregate groups, one can distinguish between sorts of morphologies based on particle characteristics. There are heterogeneities in dust-morphology due to differing mechanical activity of the source in origin, as well as, due to different media/locations of production: natural surfaces (desert) or man-made (urban). Mineralogical study indicates predominantly quartz and calcite, implying natural soil resuspension is a major source, additional minerals representing anthropogenic impact. Heavy metal distribution exhibits significant spatial heterogeneity and anisotropy in urban settings, indicating irregular and localized sources of emissions. A lack of significant seasonal variability and lack of correlation with climatic variables indicate an anthropogenic influence on heavy metals rather than environmental control factors. Lithogenic elements have a natural geological source, whereas trace metals like Pb, Zn, and Cu are closely associated with human activity from sources such as vehicular traffic and industrial emissions. This study shows that the quality of air in arid environments is a product of the relationship between natural dust and anthropogenic emissions, and anthropogenic sources increase the amount of air contamination.

ACKNOWLEDGMENTS

We thank Al-Qasim Green University for the support.

CONFLICT OF INTEREST

The authors declare that there is no conflict of interests regarding the publication of this manuscript.

REFERENCES

1. Candau, Marcolino Gomes, (30 May 1911–25 Jan. 1983), Director-General Emeritus, World Health Organization, Geneva, since 1973. Who Was Who: Oxford University Press; 2007.
2. Wang Y, Wang R, Ming J, Liu G, Chen T, Liu X, et al. Effects of dust storm events on weekly clinic visits related to pulmonary tuberculosis disease in Minqin, China. Atmos Environ. 2016;127:205-212.
3. Filonchyk M, Peterson M. Development, progression, and impact on urban air quality of the dust storm in Asia in March 15–18, 2021. Urban Climate. 2022;41:101080.
4. Sissakian VK, Al-Ansari N, Knutsson S. Sand and dust storm events in Iraq. Natural Science. 2013;05(10):1084-1094.
5. Guo J, Chai G, Song X, Hui X, Li Z, Feng X, et al. Long-term exposure to particulate matter on cardiovascular and respiratory diseases in low- and middle-income countries: A systematic review and meta-analysis. Frontiers in Public Health. 2023;11.
6. Kalaiarasan G, Kumar P, Tomson M, Zavala-Reyes JC, Porter AE, Young G, et al. Particle Number Size Distribution in Three Different Microenvironments of London. Atmosphere. 2023;15(1):45.
7. Rehman AU, Nazir S, Irshad R, Tahir K, ur Rehman K, Islam RU, et al. Toxicity of heavy metals in plants and animals and their uptake by magnetic iron oxide nanoparticles. J Mol Liq. 2021;321:114455.
8. Huang C-L, Bao L-J, Luo P, Wang Z-Y, Li S-M, Zeng EY. Potential health risk for residents around a typical e-waste recycling zone via inhalation of size-fractionated particle-bound heavy metals. J Hazard Mater. 2016;317:449-456.
9. Khan SA, Muhammad S, Nazir S, Shah FA. Heavy metals bounded to particulate matter in the residential and industrial sites of Islamabad, Pakistan: Implications for non-cancer and cancer risks. Environmental Technology and Innovation. 2020;19:100822.
10. Mahmoud N, Al-Shahwani D, Al-Thani H, Isaifan RJ. Risk Assessment of the Impact of Heavy Metals in Urban Traffic Dust on Human Health. Atmosphere. 2023;14(6):1049.
11. Talib ZR, Laffta SJ. Effect of Climate Change on Land Cover (Case study: Hilla District). Journal of Engineering. 2024;30(8):136-148.
12. Mahato MK, Singh AK. Evaluation of atmospheric dust deposition rates and their mineral characterization in copper and iron mining areas, Singhbhum, India. Journal of the Air and Waste Management Association. 2020;70(12):1378-1389.
13. Wu C, Lin Z, Shao Y, Liu X, Li Y. Drivers of recent decline in dust activity over East Asia. Nature Communications. 2022;13(1).
14. Stetsenko SE, Yastrebova NA. The Influence of Urban Planning and Building Factors on The Dustiness of The Urban Environment. IOP Conference Series: Materials Science and Engineering. 2018;463:032031.

15. Athab AH, Al-Safy AH, M. Hussain KA. Comparative study of the protective role of ashwagandha nanoparticles for female albino rats treated with paraben preservative. ASEAN Journal of Psychiatry. 2024:01-04.
16. Querol X. PM10 and PM2.5 source apportionment in the Barcelona Metropolitan area, Catalonia, Spain. Atmos Environ. 2001;35(36):6407-6419.
17. Huang X, Gao W, Foroutan H. Impact of topographic wind conditions on dust particle size distribution: insights from a regional dust reanalysis dataset. Atmospheric Chemistry and Physics. 2025;25(17):9583-9600.
18. Buseck PR, Jacob DJ, Pósfai M, Li J, Anderson JR. Minerals in the Air: An Environmental Perspective. International Geology Review. 2000;42(7):577-593.
19. Satsangi PG, Yadav S. Characterization of PM2.5 by X-ray diffraction and scanning electron microscopy–energy dispersive spectrometer: its relation with different pollution sources. Int J Environ Sci Technol (Tehran). 2013;11(1):217-232.
20. Bora J, Deka P, Bhuyan P, Sarma KP, Hoque RR. Morphology and mineralogy of ambient particulate matter over mid-Brahmaputra Valley: application of SEM–EDX, XRD, and FTIR techniques. SN Applied Sciences. 2021;3(1).
21. Wittmaack K. Brochosomes produced by leafhoppers-a widely unknown, yet highly abundant species of bioaerosols in ambient air. Atmos Environ. 2005;39(6):1173-1180.
22. Measuring the Trace Elemental Composition of Size-Resolved Airborne Particles. American Chemical Society (ACS).
23. Li WJ, Shao LY. Observation of nitrate coatings on atmospheric mineral dust particles. Atmospheric Chemistry and Physics. 2009;9(6):1863-1871.
24. Shiva Nagendra SM, Diya M, Chithra VS, Menon JS, Peter AE. Characteristics of air pollutants at near and far field regions of a national highway located at an industrial complex. Transportation Research Part D: Transport and Environment. 2016;48:1-13.
25. Panda S, Shiva Nagendra SM. Chemical and morphological characterization of respirable suspended particulate matter (PM10) and associated heath risk at a critically polluted industrial cluster. Atmospheric Pollution Research. 2018;9(5):791-803.
26. Mico S, Deda A, Tsaousi E, Alushllari M, Pomonis P. Complex refractive index of aerosol samples. AIP Conference Proceedings: AIP Publishing; 2019. p. 060002.
27. Ram SS, Kumar RV, Chaudhuri P, Chanda S, Santra SC, Sudarshan M, et al. Physico-chemical characterization of street dust and re-suspended dust on plant canopies: An approach for finger printing the urban environment. Ecological Indicators. 2014;36:334-338.
28. Conradi JC. Howard Pospesel. Introduction to logic. Propositional logic. Prentice-Hall, Inc., Englewood Cliffs, N.J., 1974, xii + 211 pp. - Howard Pospesel. Introduction to logic. Predicate logic. Prentice-Hall, Inc., Englewood Cliffs, N.J., 1976, xiii + 205 pp. Journal of Symbolic Logic. 1978;43(2):383-383.
29. Sparks DL. Environmental Soil Chemistry: An Overview. Environmental Soil Chemistry: Elsevier; 2003. p. 1-42. http://dx.doi.org/10.1016/b978-012656446-4/50001-3
30. Tao Z, Guo Q, Wei R, Dong X, Han X, Guo Z. Atmospheric lead pollution in a typical megacity: Evidence from lead isotopes. Sci Total Environ. 2021;778:145810.
31. Bourliva A, Papadopoulou L, Aidona E. RARE ELEMENTS (ZR, NB, LA, CE AND HF) IN TRAFFIC EMITTED FERRIMAGNETIC PARTICLES FROM ROAD DUSTS. Bulletin of the Geological Society of Greece. 2017;50(4):2100.
32. Xavier JR, Vinodhini SP, Raja Beryl J. Innovative multifunctional nanocomposite coated aluminum alloy for improved mechanical, flame retardant, and corrosion resistance in automobile industries. The Journal of Adhesion. 2024;101(4):660-705.
33. Croffie MET, Williams PN, Fenton O, Fenelon A, Daly K. Rubidium measured by XRF as a predictor of soil particle size in limestone and siliceous parent materials. J Soils Sed. 2021;22(3):818-830.
34. Dai J-L, Zhang M, Zhu Y-G. Adsorption and desorption of iodine by various Chinese soils. Environ Int. 2004;30(4):525-530.
35. Shinonaga T, Gerzabek MH, Strebl F, Muramatsu Y. Transfer of iodine from soil to cereal grains in agricultural areas of Austria. Sci Total Environ. 2001;267(1-3):33-40.
36. Toxicological profile for lead. Agency for Toxic Substances and Disease Registry; 2020 2020/08.
37. Sugawara Y, Araake K, Muto I, Takahashi M, Matsumoto M, Hara N. Effect of Phosphate and Chromate Pigments on Sacrificial Corrosion Protection by Al–Zn Coating and Delamination Mechanism of Pre-painted Galvalume Steel. ISIJ Int. 2016;56(12):2267-2275.
38. Tiwari P, Gupta S, Shankar S, Srivastava P, Mehrotra BJ, Srivastava MK, et al. Integrated mineral identification of PM10 using XRD, ATR-FTIR and SEM–EDX techniques in Indo-Gangetic Plain (IGP) and Indo-Himalayan Region (IHR). Environmental Monitoring and Assessment. 2025;197(8).
39. Guda AM, El Kammar AM, Abu Salem HS, Abu Khatita AM, Mohamed MA, El-Hemaly IA, et al. Integrated geochemical and magnetic potentially toxic elements assessment: a statistical solution discriminating anthropogenic and lithogenic magnetic signals in a complex area of the southeast Nile Delta. Environmental Monitoring and Assessment. 2024;196(3).
40. Liu P, Han X, Chao S, Lu X, Wang Z, Yang Y, et al. Identification of priority factors for risk control of trace toxic elements in surface resuspended dust of university campuses. Sci Rep. 2024;14(1).
41. Ulutaş K. Risk assessment and spatial distribution of heavy metal in street dusts in the densely industrialized area. Environmental Monitoring and Assessment. 2022;194(2).
42. Tang R, Ma K, Zhang Y, Mao Q. The spatial characteristics and pollution levels of metals in urban street dust of Beijing, China. Appl Geochem. 2013;35:88-98.
43. Wan D, Han Z, Yang J, Yang G, Liu X. Heavy Metal Pollution in Settled Dust Associated with Different Urban Functional Areas in a Heavily Air-Polluted City in North China. International Journal of Environmental Research and Public Health. 2016;13(11):1119.
44. Aljewari AFM, Al-Salman IMA. Evaluation of Heavy Metals Concentration in Street, Storm and Suspended Dust in Al-Zafaraniya Area, Baghdad- Iraq. Ibn AL-Haitham Journal for Pure and Applied Sciences. 2023;36(1):1-14.